International Conference on Space Optics—ICSO 2008

Toulouse, France

14–17 October 2008

Edited by Josiane Costeraste, Errico Armandillo, and Nikos Karafolas

LIDAR technology developments in support of ESA Earth observation missions

Yannig Durand

Jérôme Caron

Arnaud Hélière

Jean-Loup Bézy

et al.

International Conference on Space Optics — ICSO 2008, edited by Josiane Costeraste, Errico Armandillo, Nikos Karafolas, Proc. of SPIE Vol. 10566, 105661F · © 2008 ESA and CNES
CCC code: 0277-786X/17/$18 · doi: 10.1117/12.2308264

LIDAR TECHNOLOGY DEVELOPMENTS IN SUPPORT OF ESA EARTH OBSERVATION MISSIONS

Yannig Durand[(1)], Jérôme Caron[(1)], Arnaud Hélière[(1)], Jean-Loup Bézy[(1)], Roland Meynart[(1)],

Directorate of Earth Observation Programmes, European Space Agency, P.O. Box 229, 2200 AG Noordwijk (the Netherlands) tel: 31715653496 fax: 31715654696 email: Yannig.Durand@esa.int

ABSTRACT

Critical lidar technology developments have been ongoing at the European Space Agency (ESA) in support of EarthCARE (Earth Clouds, Aerosols, and Radiation Explorer), the 6th Earth Explorer mission, and A-SCOPE (Advanced Space Carbon and Climate Observation of Planet Earth), one of the candidates for the 7th Earth Explorer mission. EarthCARE is embarking an Atmospheric backscatter Lidar (ATLID) while A-SCOPE is based on a Total Column Differential Absorption Lidar. As EarthCARE phase B has just started, the pre-development activities, aiming at validating the technologies used in the flight design and at verifying the overall instrument performance, are almost completed. On the other hand, A-SCOPE pre-phase A has just finished. Therefore technology developments are in progress, addressing critical sub-systems or components with the lowest TRL, selected in the proposed instrument concepts.

The activities described in this paper span over a broad range, addressing all critical elements of a lidar from the transmitter to the receiver.

1. INTRODUCTION

Established in the mid-1990s, ESA's Living Planet Programme has recently reformulated the most important Earth science questions to be addressed in the years to come. Concerning the strategy outlined for the observational challenges of the atmosphere, the document recalls the need of more detailed observations on dynamics, thermodynamics and chemical composition, of more advanced measurements with better spatial and temporal resolution, of sustainability of observations of wind and Earth's radiation budget and of a better characterization of clouds and precipitations [1].

A lidar bringing its own lighting to its target, independently of the natural sources of light, provides a new kind of powerful measurement technique matching the needs above mentioned. In space, a lidar can probe continuously with high accuracy and resolution and with global coverage the structure of the Earth atmosphere as well as some parameters of land and sea surface.

The development of advanced lidar systems for space applications and their evaluation by airborne or ground based test campaigns is considered an important strategic element of the ESA Earth Observation Programme. Since the early eighties, ESA has been supporting the development of the critical subsystems of any lidar, namely lasers and detectors. Three missions, embarking three different kinds of lidars and currently in different phases of implementation, underline the successful approach followed by ESA in the lidar risk mitigation activities. These missions are ADM-Aeolus [2] in Phase C/D embarking ALADIN, a Doppler Wind Lidar, EarthCARE [3] in Phase B with a payload encompassing an Atmospheric backscatter Lidar (ATLID) and A-SCOPE [4] in Phase 0, the payload of which is based on a Differential Absorption Lidar.

2. EarthCARE

2.1 Mission

The EarthCARE mission is the 6th Earth Explorer mission of ESA's Living Planet programme. The EarthCARE mission has been specifically defined with the objective of improving the understanding of cloud-aerosol-radiation interactions in order to include them correctly and reliably in climate and numerical weather prediction models. The goals are to retrieve vertical profiles of clouds and aerosols, and the characteristics of their radiative and micro-physical properties to determine flux gradients within the atmosphere and fluxes at the Earth's surface, as well as to measure directly the fluxes at the top of the atmosphere and also to clarify the processes involved in aerosol-cloud and cloud-precipitation-convection interactions. The mission consists on a suite of four instruments, active and passive, embarked on the same satellite: an ATmospheric backscatter LIDar (ATLID), a Cloud Profiling Radar (CPR), a Multi-Spectral Imager (MSI) and a Broad Band Radiometer (BBR). The satellite flies on a Sun-synchronous orbit at about 400 km altitude.

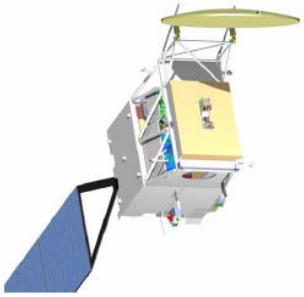

Fig. 1. EarthCARE spacecraft accommodation

ATLID, the atmospheric lidar, is composed of a single wavelength lidar with a High-Spectral Resolution (HSR) receiver separating the spectrally broaden Rayleigh (molecular) and narrow band Mie (cloud and aerosol particles) backscatter returns. An additional Mie cross-polarisation channel is implemented. Table 1 summarizes the observation requirements applicable to ATLID from -0.5 up to 40 km altitude range.

Table 1. ATLID observation requirements

	Mie co-polar channel	Rayleigh channel	Mie cross-polar channel
Cirrus optical depth	0.04		
Backscatter sr^{-1} m^{-1}	$8\ 10^{-7}$		$2.6\ 10^{-5}$
Vertical resolution	100 m	300 m	100 m
Horizontal resolution	10 km		
Required Accuracy	50%	15%	45%

ATLID transmitter operates at the third harmonic of a Nd:YAG laser around 355 nm. This wavelength allows moderate pulse energy to be used without exceeding eye safety constraints. A conventional design made of a low power oscillator and a power amplifier is implemented. The Mie-Rayleigh separation is performed by a high resolution Fabry-Pérot étalon. The HSR technique uses the reduction in the molecular return to directly determine the extinction of aerosols and thin clouds, which is then used to correct the backscatter coefficient in the Mie channel for attenuation, and find the extinction to backscatter ratio of the lidar signal. CCD's are considered as detectors. A wavelength tuneable laser ensures in-flight relative calibration of the aerosol channel and of the molecular channel and possibly, for Earth Doppler compensation. Table 2 lists the main characteristics of the lidar, resulting in an instrument of about 300 kg and 500 W.

Table 2. ATLID design parameters

Parameters	Unit	Values
Laser pulse energy @ 355 nm	mJ	30
Pulse Repetition Frequency	Hz	74
Spectral line width (FWHM)	MHz	50
Telescope diameter	m	0.6
HSR etalon bandwidth	pm	0.35
Detector		CCD

Following the selection for implementation of the EarthCARE mission and the development risk analysis performed during phase A, in 2005 a pre-development programme was undertaken to reduce the technical and programmatic risks of the mission. Even though ATLID inherits from the ALADIN development, the pre-development programme has mainly focussed on critical aspects of the lidar. It encompasses the development and test of laser sources, acquisition chains, high-power laser diodes and detectors.

2.2 ATLID Laser Source (ATLAS)

ESA has conducted two parallel developments of laser transmitters aiming at enabling the technology of an efficient frequency tripled Nd:YAG laser. The pre-development activities consisted in proposing a Flight Model (FM) laser concept and in designing, manufacturing and testing the transmitter in a configuration as close as possible to the FM one. The tests aimed at demonstrating the validity of the design, of the modelling tools and at bringing experimental support for further optimizations of the flight configuration to be designed in the current phase B.

Table 3. ATLAS performance requirements

Parameters	Requirements
Output energy	23mJ/100 Hz or 30mJ/70 Hz
Optical – optical efficiency	6% (8 % target)
Energy short term stability	< ±10% over 1.4sec
Spatial quality	$M^2 < 4$
Pulse duration	< 35ns
Longitudinal mode	Single
Pulse linewidth	< 50MHz
Spectral purity	99% in 100MHz
Frequency stability over 1.4 sec	< 10MHz rms

The specifications, listed in Table 3 target a laser with emphasis on a much improved optical to optical efficiency compared to ALADIN transmitter. A goal of 8 % was envisaged at the beginning of the activity. Two different concepts have been retained, both based on a master oscillator / power amplifier configuration (MOPA) and longitudinal end pumping to improve the efficiency [5,6].

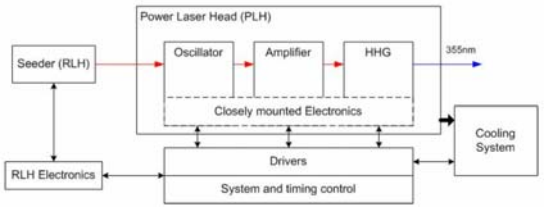

Fig. 2. Functional block diagram of ATLAS.

The overall architecture for both concepts is shown in Fig. 2. A reference laser delivers the seed wavelength to the oscillator. The tuneable reference laser is not considered as critical as it is a recurrent item manufactured and already space-qualified for ALADIN. The oscillator is part of the power laser head which comprises as well the amplifier section and the harmonic stages (second and third harmonic generation). The main design drivers for such a laser are the required efficiency and the lifetime (3 years in orbit). The optical to optical efficiency is divided into the conversion from the 808 nm pump source to the

1064 nm laser optical output and the conversion from the 1064 nm into the required 355 nm. Laser manufacturers have focused their design effort to optimize these two efficiencies. The requirement on the lifetime is equivalent to 10 GShots and drives the derating and redundancy strategies.

The cavity control for such a laser could be based either on pulse measurements, or on measurement of the transmitted or reflected cw seed laser light. Methods using pulse properties, e.g. pulse build up time or heterodyne frequency are limited by the pulse repetition frequency of about 100 Hz. As micro vibrations can reach higher values, such methods are not suitable and both concepts have relied on direct measure of the cavity length by evaluating the Fabry-Perot resonance properties of the cavity. The cavity dither method was selected as baseline based on its simplicity and its performance sufficient for the purpose of ATLAS: stability of the frequency was found below 1 MHz in the infra-red when no disturbance was applied on the cavity and below 3 MHz when either a 20 nm disturbance at 400 Hz or a 500 nm disturbance at 1 Hz was applied on the cavity by a piezo actuator dithering the output coupler mirror.

One laser concept relies on the patented InnoSlab technology. The slab crystal is partially end pumped from one or two sides. Thanks to the fact that only two sides of the crystal need to be optically polished, the heat dissipates efficiently and homogeneously over the two metal heat sink soldered to the large faces of the slab. The four optically unused surfaces on the crystal are roughened to prevent internal parasitic laser oscillations. To operate the InnoSlab laser as amplifier, the beam is folded in a single pass configuration through the crystal and widened with every pass so that the fluence can be kept constant and remains far below the damage threshold (see Fig. 3).

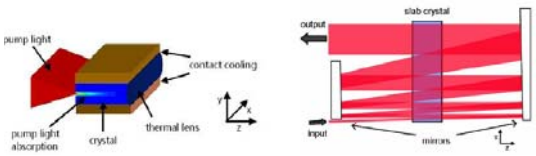

Fig. 3. Innoslab concept (left); beam path of the a InnoSlab folded single path amplifier (right)

Pumping is achieved with coupling many fast-axis collimated laser bars via a homogenizer to form a rectangular gain cross section inside the slab. The pump light homogenization enables homogeneous intensity distribution even at failure of a whole or several diode bars.
In the first phase of the development, geometrical parameters of the laser design have been simulated and experimentally optimized (doping concentration, crystal length, mirror curvature, cavity length…). At the end of this phase, all specifications could be met, resulting in about 25 mJ in the UV with an optical to optical efficiency of 8 %. Excellent beam quality, spectral properties and energy shot-to-shot stability were obtained. Further tests to explore the limits of the laser configuration were conducted. Optical output energy in the UV of 34 mJ could be achieved by reducing beam diameter which implied third harmonic generation (THG) efficiency higher than 50 % (see Fig. 4) and overall optical to optical efficiency higher than 10 %. However in such configuration, the maximum peak intensity on the LBO crystal end surface was higher than 300 MW/cm^2, which decreases the reliability of the laser.

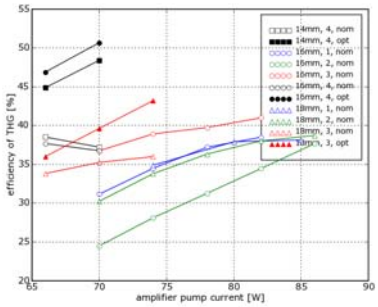

Fig. 4. Optimisation of the THG efficiency for different LBO crystal lengths (shape), number of lenses in the telescope before the crystal (colour) and the crystal temperature (hollow or filled dots).

Following the phase of optimization of the geometrical parameters, a compact design (400 mm * 200 mm) of the oscillator has been completed (see Fig. 5).

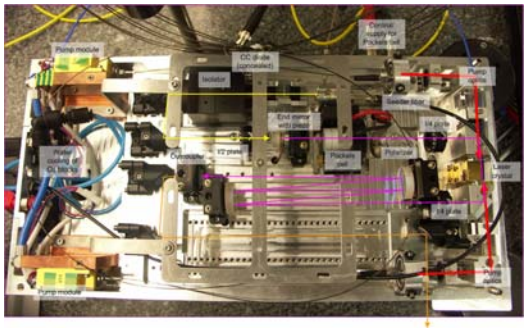

Fig. 5. Compact setup of the oscillator with pumping section in red, seeding path in yellow and cavity path in purple

Following the performance tests activities, the initially proposed FM concept has been iterated to include the lessons learned. The resulting preliminary design of the FM pressurised laser includes the following features:

- High efficiency

- Long lifetime thanks to pump diode and tripler crystal redundancy
- Pressurized housing with symmetric shape, mechanically decoupled from the optical baseplate
- High thermal stability by use of loop heat pipes

The second ATLAS concept depicted in uses an injection-seeded Q-switched master oscillator followed by a pre-amplifier and a power amplifier. The low power oscillator is designed to emit single-longitudinal mode >15 mJ pulses with ~25 ns FWHM pulse duration, in order to fulfill the pulse duration specification of at the 355 nm output. The MO is longitudinally-pumped with one laser diode stack. The stack is collimated by micro lenses array, corrected for aberration by a phaseplate and then focused inside the rod. A cold redundancy based on polarization coupling insures the lifetime.
The amplifiers are end-pumped by two collimated stacks (plus a cold redundancy) identical to those used in the MO pump section. Two-pass amplifiers are implemented using polarisation decoupling with polariser and quarter waveplate.

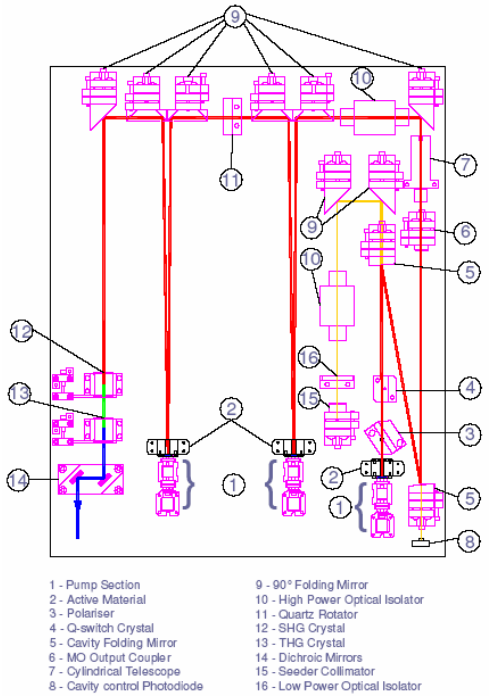

Fig. 6. Opto mechanical scheme of the ATLAS PDM with seeding path in yellow and main laser path in red

For the harmonic section several configurations with most suitable non-linear crystal were analyzed (LBO, BBO, BiBO and KTP). From the simulation of the efficiency, the LBO type II was selected as third harmonic generation and tests were performed to compare LBO type I, BBO and BiBO as the second harmonic generation crystal. The optimal conversion efficiency of 31 % was finally achieved with the LBO type I as SHG and LBO type II as THG. All performance parameters were within the specification except the UV energy which could reach 24 mJ only in multi longitudinal mode. Indeed during SLM operation, spatial hole burning prevented from extracting all the stored energy. The UV energy stability measured over 1.4 s shows a standard deviation of 0.14 % as seen in Fig. 9. Frequency stability over 5 minutes is below 1.5 MHz in the IR.

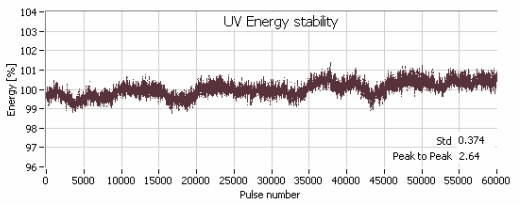

Fig. 7. UV energy stability measured for 10 minutes

2.3 Laser diodes

In view of the increase lifetime and efficiency required for ATLID, it was deemed necessary to initiate several activities not only aiming at assessing but also at developing passively cooled high power laser diode arrays (stacks) specifically suited for the requirements of space operation. An essential requirement supporting the lifetime need, but also supporting the overall wall-plug efficiency of the transmitter is the electro-optical efficiency of the stack. It is required to stay higher than 50 % during the lifetime of the devices. EOL is reached when either output power decreases below 700 W or efficiency decreases below 50 %. Other specifications are an optical output power of 700 W and some stringent geometrical requirements at bar level in order to allow a proper collimation of the optical beam as could be required by the flight laser design. The main specifications are presented in Table 4. Environmental (thermo-mechanical tests, vacuum compatibility and radiation tests) and endurance tests of at least half the required lifetime will conclude these developments.

Table 4. Specifications of the long lifetime stacks

Parameters	Specifications
Wavelength	(807 ± 2) nm
Peak output power	> 700 W
Pulse width	150-200 µs
Repetition rate	70-100 Hz
Total efficiency	> 50%
Emitting area	< 10 mm x 14 mm
Lifetime	10 billion shots
Pitch	0.4-1.7 mm

Two parallel developments are on-going. One relies on the heritage developed for ALADIN, the second one

proposes an innovative approach deemed interesting to pursue. Both developments aim at reaching a reproducible and reliable manufacturing process.
The development based on the ALADIN heritage has introduced major changes from the bars manufacturing to the final step of the stacking. The pitch between bars has been increased to allow a better control of the geometrical parameters and to minimize the thermo-mechanical constraints in the bars. The number of bars per stack has been decreased to 9 while the power per bar slightly increased to 80 W. The overall epitaxy and geometry of the bars insure that the electro-efficiency requirement is met. At the beginning of life, efficiency as high as 60 % has been demonstrated as seen in Fig. 8. Based on the finding of a Failure Mode and Effect Analysis the tooling and handling of the stacks has been much improved. Three different stack designs have been selected and tested in support of the Critical Design Review showing almost unchanged electro-optical characteristics even after 3 Gshots (see Fig. 9).

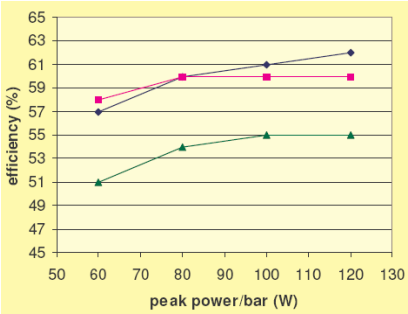

Fig. 8. Electro-optical efficiency vs the optical power per bar for different single bars on a stack package; triangle: 80 % Field Factor (FF) and 0.9 mm Cavity Length (CL), square: 50 % FF 0.9 mm CL, circle: 50 % FF 1.2 mm CL.

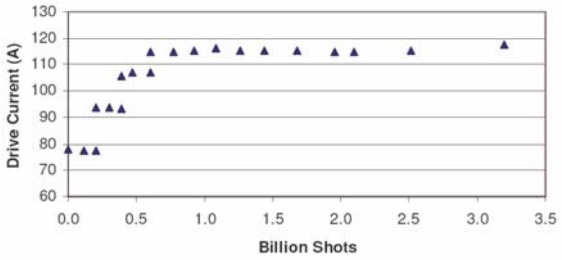

Fig. 9. endurance pre-test of a 4 bars stack built with one of the 3 selected designs showing no degradation at 115 W/bar.

One design has been selected and 24 stacks have been manufactured to populate endurance tests in air and in vacuum. After burn-in, the average efficiency amounted to 58 % and all other acceptance criteria were met. Near-field pictures revealed very few dead emitters evidencing the robustness of the new design.

Fig. 10. Near-field picture of one 9 bars stack after burn-in, taken on the atmospheric endurance test bench

In vacuum the endurance test has started with 6 stacks. The vacuum test chamber has been equipped with a integrating sphere which can be positioned on top of each stack. Measurement can therefore be performed during the endurance test, without disrupting the vacuum or disassembling the stack from its support. Up to now, no degradation is observed after 2000 hours, i.e. about 750 Mshots as reported in Fig. 11.

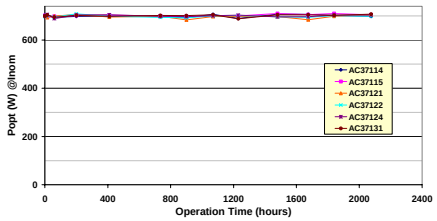

Fig. 11. Optical power measured at 25 deg for 6 stacks running in vacuum.

In the second development, a novel stacking approach is assessed. Bars type has been selected among high performing but commercial bars. Care was taken to optimize the load per bar while insuring the electro-optical requirements of Table 4. Indeed electro-optical efficiency depends of both the resonator length and the fill factor. With the choice of the laser bar material a compromise needs to be taken since lowest possible facet load, lowest possible current density and highest efficiency are conversed influenced by filling factor and resonator length. To gain confidence in the reliability of the selected bars, preliminary endurance tests have been run showing almost no degradation after 2 Gshots under a high load of more than 200 W per bar.

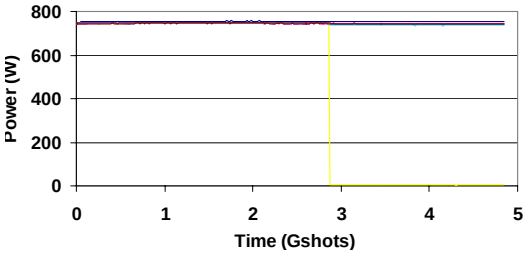

Fig. 12. Optical power of 12 stacks in endurance at 25 degrees under atmospheric condition

All materials used in the stack are thermally expansion matched to minimize the ageing effect due to stress and expansion mismatch in the laser bar. A large pitch has been selected to improve the heat transfer into the heat sink. All required parameters of the 8 bars stacks, but the polarization, have been met. Following a successful burn-in which included environmental tests at acceptance level, 12 stacks in air and 10 stacks in vacuum have started endurance tests under two duty cycles. The nominal duty cycle of 2% will allow the stack to reach half the required lifetime, and an increased duty cycle of 4 % will allow accumulating the number of shots required by the mission within 18 months. In air, the accelerated stacks have already reached more than 5 Gshots without sign of degradation of their electro-optical properties as is evidence for instance on the behaviour of the output optical power displayed in Fig. 12. Only one failure is reported due to a burn mosfett. Under vacuum, the tests have been interrupted after 1 month operation due to a rapid decay of the optical power. Failure investigation is ongoing to better understand the causes of this behaviour.

2.4 ATLID Filtering and Acquisition chain

The Atmospheric Lidar Filtering and Acquisition (ALFA) programme consists in the pre-development of the lidar receiver critical sub-systems as the filtering stage, the detector and the acquisition chain, the verification of the receiver functions and performance with appropriate Optical Ground Support Equipment.
The core of one activity consisted in tunable and capacitance stabilized high resolution Fabry-Perot etalons breadboarding, extensive optical characterisation of the whole filtering chain and mechanical assessment of the etalons through mechanical vibrations testing (see Fig. 13). High peak transmission, higher than 70%, together with high finesse, 33, have been demonstrated. The pre-development activity included as well the assessment and pre-qualification of enhanced photomultiplier tubes and the consolidation of the acquisition chain.

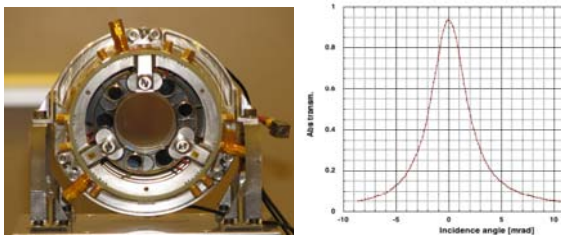

Fig. 13. Tuneable Fabry-Perot etalon under mechanical test and high peak transmission curve demonstrated through this development.

A second activity aimed at validating the optical performance of non-tuneable and high transmission Fabry-Perot etalons, investigating the performance of an optical fibre link, assessing a lidar detector based on E2V L3 technology together with its acquisition chain.
The activities are completed and have been successful in demonstrating high optical performance of the etalons and fibres.

2.5 ATLID Detectors

The pre-development programme included first the demonstration of electron-multiplication CCDs devices (so-called L3CCD of E2V Technology) optimized for fast sampling of lidar signals at very low noise. This included demonstration of its suitability for use in a space radiation environment. High electro-optical performance has been demonstrated, although some limitations have been shown in linearity and charge transfer efficiency, especially after irradiation. Iteration on the detector design is believed to overcome this issue.

Based on the outcomes of the ALFA pre-development, new activities have been initiated in order to demonstrate the baseline detector performance, called Memory CCD. Fast sampling of the echo signal (1.5 MHz corresponding to 100 m vertical sampling distance), on-chip storage of the echo samples, and an innovative read-out stage, should enhance the acquisition chain radiometric performance. The pre-development activity aims at manufacturing a prototype of the Memory CCD and validating its performance under representative environment. Additionally, the read-out performance has to be demonstrated through breadboarding.

3. A-SCOPE

3.1 Mission

As outcome of the call for the 3rd cycle of Earth Explorer missions, two DIAL lidars have been proposed. One proposed lidar aims at measuring CO_2 in the atmosphere (A-SCOPE). The second proposed lidar targeted measurement of atmospheric water vapour as part of the so-called Space-Wave mission. As result of an ESA review, only A-SCOPE has been retained as one candidate for the next series of Earth Explorer mission to be launched end of 2016. The A-SCOPE mission aims at improving our understanding of the global carbon cycle and at the determination of carbon fluxes at regional scale through the near-global measurement of column averaged dry air CO_2 mixing ratio to high precision and with low bias error. Observation requirements are summarised in Table 5.

Table 5. A-SCOPE observation requirements

Parameters	Requirements		
Level 1b product	Total differential atmospheric optical depth		
Vertical resolution	Total column		
Integration length	50 km		
Relative Random error		Threshold	Target
	@ 1.57μm	$2.2\ 10^{-3}$	$7.4\ 10^{-4}$
	@ 2.05 μm	$4.5\ 10^{-3}$	$1.5\ 10^{-3}$
Relative Systematic error	10% of random error		
Scattering surface elevation accuracy	3 m		

Coverage and accuracy are the key performance parameters of A-SCOPE as compared to other CO_2 missions. Measuring carbon dioxide mixing ratio from space is challenging because of its globally low concentration in the atmosphere (on average approximately 380 ppm in volume). The measurement of CO_2 gradients and temporal variations is even more difficult as CO_2 is relatively homogeneous in the atmosphere, with maximum variations of tens of ppm. The atmospheric backscatter signal is too weak to allow vertically resolved measurement with the current laser technology. The most promising way to achieve an accurate measurement from space is to integrate the whole atmospheric column relying on the echo from the backscattering surface (ground, canopy or thick clouds). Such measurement technique is called Integrated Path Differential Absorption (IPDA). The A-SCOPE lidar instrument transmits two laser pulses at slightly different wavelengths. One laser wavelength (on-line) is selected within a CO_2 absorption line while the other wavelength (off-line) is selected close to the first one but with sufficient separation to encounter a significantly smaller absorption. The ratio of the return signals correlated with the associated transmitted laser energy gives a measurement of the CO_2 Differential Absorption Optical Depth (DAOD). From the DAOD, the column-averaged dry air CO_2 mixing ratio is calculated using the hard target DIAL equation with ancillary atmospheric and spectroscopic data. Sizing of the lidar is dictated by the random error requirements of 0.5 ppm for the CO_2 mixing ratio (threshold of 1.5 ppm). Systematic errors contributing to spatial or temporal biases have to be 10 % lower. Table 6 summarises the main technical specifications of the A-SCOPE instrument for both concepts proposed at the end of the pre-Phase A studies.

The space segment consists of a single satellite in a near-polar sun-synchronous orbit at a mean altitude in the range of 350-400 km and operating a near-nadir pointing IPDA lidar.

Table 6. A-SCOPE design parameters

Parameters	Unit	Values	
Wavelength	nm	1572	2051
Laser pulse energy	mJ	50	55
Pulse Repetition Frequency	Hz	50	
Spectral stability (drift)	kHz	70	100
Telescope diameter	m	1	1.2
Detector		APD	

For the latter two different concepts have been assessed, operating at wavelengths around 1.57 μm and 2.05 μm respectively (see Fig. 14). Developments have been initiated for suitable laser sources and detectors at these wavelengths.
The driving requirement for the A-SCOPE instrument is the requirement on Systematic Error. It drives the design of the radiometric calibration system, receiver architecture, detector linearity, frequency stability and spectral purity of the transmitter as well as the pointing stability

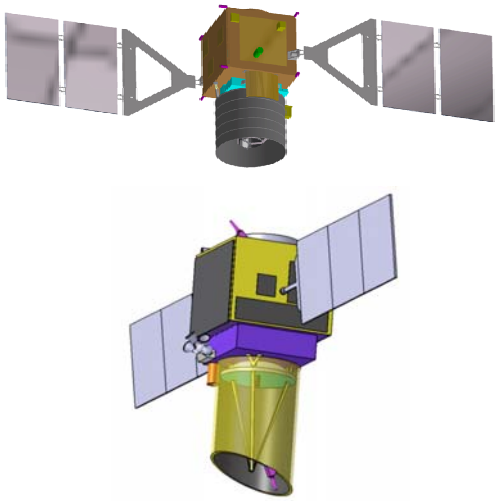

Fig. 14. A-SCOPE spacecraft configuration with IPDA lidar concept at 2.05 μm (top) and 1.57 μm (bottom)

A bistatic configuration is proposed as it offers the advantage of polarization insensitivity and a complete decoupling of the receiver from the transmitter. The receiver optical subsystem is based on a 1 m class Cassegrain-like telescope and avalanche photodiode detector. For each of the bands, a candidate laser source has been selected. Both options need the generation of a pair of pulses (on- and off-line wavelengths) separated by about 250 μsec at an overall pulse repetition frequency of 50 Hz. For the generation of double pulses at 1.57 μm with 50 mJ energy per pulse, the Nd:YAG MOPA (Master Oscillator, Power Amplifier) laser at 1.06 μm combined with an OPO/OPA (Optical Parametric Oscillator/Amplifier) as frequency converter is preferred. For the generation of

double pulses at 2.05 µm with 55 mJ energy per pulse, the same approach or a direct emission laser based on a Thulium (Tm) pumped Holmium (Ho) power oscillator can be implemented.

3.2 NIR laser sources

A promising NIR transmitter concept meeting the A-SCOPE requirements is a frequency converter based on a MOPA arrangement. At 2.05 µm, the development aimed at delivering pulses of 40 mJ at 50 Hz with more than 30 % optical to optical conversion efficiency.
Both Raman shifting scheme and parametric frequency conversion scheme (e.g. an Optical Parametric Oscillator OPO) have been investigated. Following trade-off studies of both techniques, the implementation of an entangled cavity, doubly resonant OPO has been selected as it delivers a tunable single mode emission at any wavelength (from 1.5 to 4.3 µm) from a robust and compact arrangement.

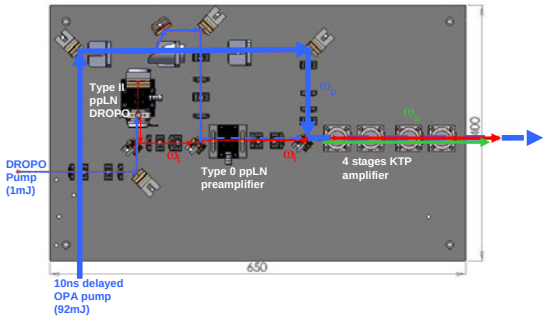

Fig. 15. MOPA overall design

Regarding the amplification stage, type 0 ppLN has been selected for the preamplifier and type II KTP crystals have been selected for the booster stage. In order to optimize the temporal overlap between the signal wave emitted by the OPO and the OPA pump, a 10 ns delay line is built-up. For the frequency tuning and locking of the wavelength, two options have been investigated. The first one uses a high finesse wavemeter to monitor the 2 µm radiation after frequency doubling; with this approach, frequency stabilization within a few MHz in a shot-to-shot basis is expected. The second approach is based on the development of a differential Helmholtz resonator cell, which performances depend on the signal to noise ratio that is achieved. A breadboard has been setup demonstrating around 11 mJ of signal for 86 mJ of pump incident on the KTP crystals and a total pump energy used of 93 mJ. An overall conversion efficiency of 12 % is thus obtained for the signal beam alone. High signal beam quality is achieved with M2 value better than 1.9 for both horizontal and vertical directions. For frequency characterization, a high Finesse wavemeter, that can measure the frequency with 1 MHz precision, shows the frequency stabilisation of the signal wave with a measured standard deviation of 3 MHz over 30 s.

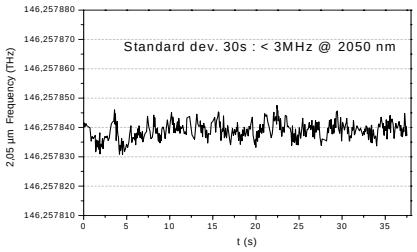

Fig. 16. Time recording of the signal frequency.

At 1.57 µm a development of a more conventional OPO/OPA has been initiated that has to fulfil the technical specifications of the A-SCOPE transmitter: spectral and spatial properties in conjunction with proper pulse energy. Following a first theoretical trade-off phase concerning the crystal material, KTP has been retained as the most suitable crystal w.r.t. other crystals such as KTA, LiNbO3 and KNbO3. In the design phase, a promising concept based on an injection seeded low power OPO whose radiation will then be amplified by means of a high power optical parametric amplifier system, has been retained.

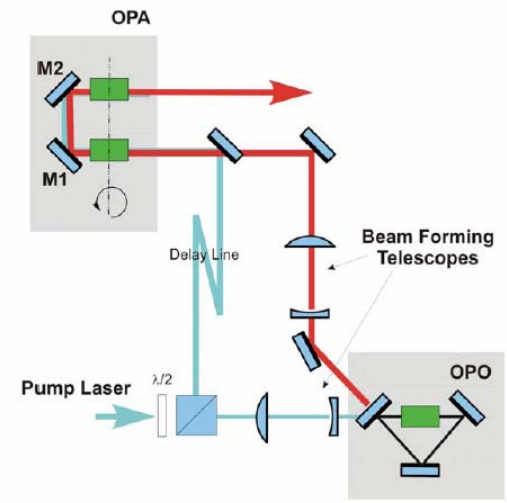

Fig. 17. Optical layout of the OPO/OPA arrangement

The low-power oscillator design has to be chosen so that it provides an optimum beam profile which is generally achievable near oscillation threshold and that can be maintained through the amplification process. The technique of injection seeding will guarantee that the parametric devices emit in a narrow bandwidth with the highest possible spectral purity. Up to now a KTP-OPO has been setup and several KTA-OPA

designs will be tested. Energies up to 24 mJ have been obtained with a non-optimised pump laser. Coupling of a more intense pump laser, improvement of the optomechanical design and of the pointing stability together with a fifth KTA crystal should allow to reach the required 50 mJ.

An attractive alternative to the generation of 2 μm is based on fibre laser which exhibits very high efficiency. A development has just been initiated aiming at demonstrating the technical feasibility of a laser diode pumped all-fibre pulsed CO_2 DIAL transmitter laser based on the generation of both on- and off-lines in the 2.05 μm channel with a short time separation. Overall the averaged optical output power of the fibre laser source (FLS) shall amount to a minimum of 6 W, including both the generated on- and off- lines. At a fixed pulse repetition frequency in the range of 2 - 4 kHz the FLS shall deliver output pulses of several tens of nanoseconds pulse duration with an energy of minimum 2 mJ per pulse at the selected on-line and > 0.2 mJ at the off-line. In addition to the highly reproducible and precise absolute frequency generation the FLS output pulses shall exhibit a narrow linewidth in the range of few tens of MHz with a linewidth stability of better than 10%, a central frequency stability of better than 0.2 MHz and a spectral purity of 99.9% within 1 GHz.

3.3 NIR Detectors

A-SCOPE demanding radiometric requirements can only be achieved by using Avalanche Photodiode (APD). Such detectors being not yet commercially available at 2.05 μm, two development activities have been investigated. They address different types of material.

In the first activity, two approaches are being followed. One is based on InAlAs/InGaAs/GaAsSb type II superlattice APD with separate absorption and multiplication structure (SAM). The other is based on InAs SAM APD. Preliminary results reveal that the excess noise factor is lower for InAs devices and quantum efficiency higher. However dark current is lower for type II devices. Optimisations of the growth conditions and the passivation processes are ongoing in order to confirm whether the expected goals can be achieved.

A second activity relying on Mercury Cadmium Telluride (MCT) based APD has just been started. With MCT very low excess noise factor is expected in combination with a high gain. Preliminary performance simulation indicate that a Noise Equivalent Power smaller than 100 $fW/Hz^{0.5}$ for a detector/pre-amplifier bandwidth larger than 20 MHz is achievable.

4. CONCLUSIONS

In this paper a summary of some of the efforts initiated by ESA into the lidar technologies developments has been presented. These developments support the technical readiness of the lidar instruments planed to be flown on the coming ESA Earth Observation missions. Three Earth Explorer missions at different phases of implementation have directly benefited from the outcomes of these risk mitigation activities.

5. REFERENCES

1. *The Changing Earth – New Scientific Challenges for ESA's Living Planet Programme*, ESA-SP-1304, (2006)

2. *European Space Agency (ESA): Atmospheric Dynamics Mission, Report for Mission Selection*, ESA-SP-1233(4), (1999)

3. *European Space Agency (ESA): Earth Clouds, Aerosols and Radiation Explorer, Report for Assessment*, ESA-SP-1257(1), (2001)

4. *European Space Agency (ESA): A-SCOPE – Advanced Space Carbon and Climate Observation of Planet Earth, Report for Assessment*, To be published, ESA-SP-, (2008)

5. *ATLAS pre-development: Summary Report*, ESTEC Contract 19590/05/NL/FF

6. *ATLAS pre-development: Summary Report*, ESTEC Contract 18256/04/NL/FF

7. *Pre-development of ALFA: Summary Report*, ESTEC Contract 19506/05/NL/FF